

Discovery of an optical counterpart to the hyperluminous X-ray source in ESO 243-49

Roberto Soria^{1*}, George K. T. Hau², Alister W. Graham², Albert K. H. Kong³, N. Paul M. Kuin¹, I-Hui Li², Ji-Feng Liu⁴ and Kinwah Wu¹

¹*Mullard Space Science Laboratory, University College London, Holmbury St Mary, Surrey RH5 6NT, UK*

²*Centre for Astrophysics and Supercomputing, Swinburne University of Technology, Hawthorn VIC 3122, Australia*

³*Institute of Astronomy and Department of Physics, National Tsing Hua University, Hsinchu 30013, Taiwan*

⁴*Harvard-Smithsonian Center for Astrophysics, 60 Garden st, Cambridge MA 02138, USA*

Accepted ... Received ... in original form ...

ABSTRACT

The existence of black holes of masses $\sim 10^3$ – $10^5 M_\odot$ has important implications for the formation and evolution of star clusters and galaxies. The strongest candidate so far is the hyperluminous X-ray source HLX1, apparently located in the S0-a galaxy ESO 243-49, but the lack of an identifiable optical counterpart had hampered its interpretation. Using the *Magellan* telescope, we discovered an unresolved optical source with $R = 24.6 \pm 0.2$ mag and $V = 25.4 \pm 0.3$ mag within the X-ray error circle. This implies an X-ray/optical flux ratio ~ 1000 . Taking the same distance as ESO 243-49, we obtain an intrinsic brightness $M_R = -10.2 \pm 0.3$ mag. With the combined optical and X-ray measurements, we put constraints on the nature of HLX1. We rule out a foreground star and a background AGN. A foreground accreting neutron star is unlikely but cannot be completely ruled out. We also examined the properties of the host galaxy by combining *Swift*/UVOT observations with stellar population modelling. We found that the overall emission from ESO 243-49 is dominated by a ~ 2 –5 Gyr old stellar population, but the far-UV emission is mostly due to ongoing star-formation at a rate of $\sim 0.03 M_\odot \text{ yr}^{-1}$. There is a $\sim 15\%$ excess above the mean in the far-UV emission North East of the nucleus, towards HLX1, which we interpret as evidence of more recent or intense star formation in that region. The brightness of the optical counterpart is comparable to that of massive globular clusters. We suggest that HLX1 could be an accreting intermediate mass black hole in a star cluster. The cluster could also be the stripped nucleus of a dwarf galaxy as it passed through ESO 243-49, an event which might have caused the current episode of star formation along its trail.

Key words: galaxies: individual: ESO 243-49 – X-rays: binaries – ultraviolet: galaxies – black hole physics.

1 INTRODUCTION: ULTRALUMINOUS AND HYPERLUMINOUS X-RAY SOURCES

XMM-Newton and *Chandra* have discovered several non-nuclear X-ray sources in nearby galaxies, with luminosities up to two orders of magnitude higher than those observed from Galactic X-ray binaries. These are referred to as ultraluminous X-ray sources (ULXs; e.g., Grimm et al. 2003; Swartz et al. 2004; Roberts 2007). Those findings have challenged our current models of black hole (BH) formation and accretion. Isotropic, Eddington-limited luminosities $\gtrsim 10^{40} \text{ erg s}^{-1}$ would require BH masses $\gtrsim 100 M_\odot$, beyond the upper limit for individual stellar collapses (Yun-

elson et al. 2008). Mildly super-Eddington accretion onto particularly heavy stellar BHs ($M \sim 50 M_\odot$), and moderately anisotropic emission may explain X-ray luminosities up to $\sim \text{few} \times 10^{40} \text{ erg s}^{-1}$ without the need for more exotic astrophysical processes (Roberts 2007; King 2009).

Only a few non-nuclear sources have been observed at X-ray luminosities ≈ 0.7 – $1 \times 10^{41} \text{ erg s}^{-1}$. For example, in the Cartwheel (Wolter et al. 2006), in M 82 (Feng & Kaaret 2009), in NGC 2276 (Davis & Mushotzky 2004), and in NGC 5775 (Li et al. 2008). It is possible that such rare, extreme ULXs (sometimes known as hyperluminous X-ray sources, HLXs) may be powered by heavier BHs, formed through different channels: for example, in the collapsed core of a super star cluster, or within the nuclear star cluster of an accreted (and now disrupted) dwarf galaxy. Thus,

* E-mail: roberto.soria@mssl.ucl.ac.uk

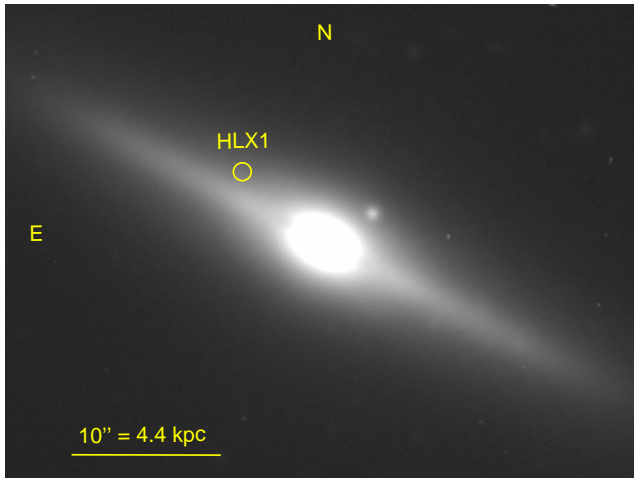


Figure 1. *Magellan/IMACS R-band* image of ESO 243-49, with the X-ray position of HLX1 marked by a circle of $0''.6$ radius.

HLXs may represent evidence of intermediate-mass BHs. However, the debate is far from settled, given the small number of HLXs known, and the possibility of confusion with background AGN. The strongest case for an intermediate-mass BH so far has been made for a recently discovered X-ray source (2XMM J011028.1–460421, hereafter HLX1: Farrell et al. 2009; Godet et al. 2009) apparently located in the galaxy ESO 243-49, or, at least, projected inside the $\mu_B = 25.0$ mag arcsec $^{-2}$ surface brightness isophote of that galaxy. Here, we report our discovery of the likely optical counterpart to this source, and our analysis of the UV emission in ESO 243-49. By determining the optical flux, and the X-ray/optical flux ratio, we test alternative models for the nature of this object. Our results strengthen the interpretation that the X-ray source belongs to ESO 243-49. We suggest that it is located inside a massive star cluster.

2 OPTICAL/UV OBSERVATIONS

ESO 243-49 is an edge-on S0-a galaxy at a luminosity distance of 91 ± 6 Mpc ($z = 0.0224$, distance modulus 34.80 ± 0.15 : Caldwell & Rose 1997). The foreground extinction is very low, $A_V = 0.043$ mag (Schlegel et al. 1998). The X-ray source HLX1 is located at RA = $01^h 10^m 28^s.27$, Dec = $-46^\circ 04' 22''.3$, based on our analysis of the source from the *Chandra* High Resolution Camera (2009 August 17). It appears projected $\approx 7''$ (≈ 3.1 kpc) to the North-East of the galactic nucleus, and $\approx 1''.8$ (≈ 800 pc) above the galactic plane. HLX1 has been detected several times with *XMM-Newton*, *Chandra* and *Swift* between 2004 and 2009 (Farrell et al. 2009; Godet et al. 2009), with an unabsorbed luminosity in the 0.3–10 keV band varying between $\lesssim 5 \times 10^{40}$ erg s $^{-1}$ and $\approx 1 \times 10^{42}$ erg s $^{-1}$. We also examined a *ROSAT/HRI* observation of the field from 1996, when HLX1 was not detected to an upper limit of $\approx 5 \times 10^{40}$ erg s $^{-1}$. Its combination of extreme luminosity (if it really belongs to ESO 243-49), soft spectrum (a thermal component at $kT \approx 0.2$ keV dominates in the highest state), and spectral changes on short timescales (Godet et al. 2009) makes it a unique object among the ULX/HLX class. Its apparent location in an S0 galaxy is also puzzling, because such galaxies are usually

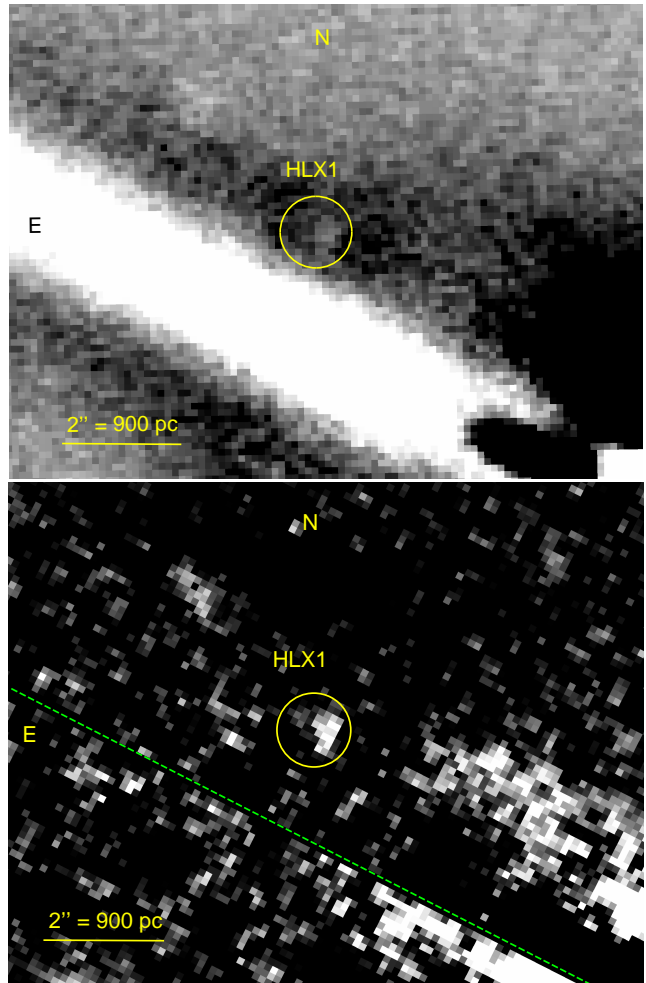


Figure 2. Top panel: differential *R-band* image of the HLX1 field, with a Gaussian-smoothed image subtracted from the original image. The X-ray position of HLX1 is marked by a circle of $0''.6$ radius. Bottom panel: *R-band* image of the same field, after the subtraction of the underlying galaxy light with the technique explained in Section 3. The location of the disk plane is marked by the dashed green line.

dominated by an old stellar population. For example, the integrated brightnesses of ESO 243-49 are $B = 14.92 \pm 0.09$ mag, $R = 13.48 \pm 0.09$ mag and $K = 10.70 \pm 0.05$ mag (from NED¹), which are indicative of a characteristic stellar age $\gtrsim 2$ –5 Gyrs. Such old populations were not previously known to host luminous ULXs or HLXs. For these reasons, it was speculated that the source might be a background AGN or a foreground neutron star, even though its X-ray properties are also very unusual for both classes of objects.

We observed the source on 2009 August 26 with the IMACS Long Camera (SITE CCD) on the 6.5-m *Baade Magellan* telescope. We took a series of 3×180 s exposures in each of the Bessell *B, V, R* filters² (Bessell 1979). The seeing was $\approx 0''.7$, and the airmass was ≈ 1.2 . For the UV band, we used the 30-cm UV/Optical Telescope (UVOT) on board *Swift*, which has observed the target several times between

¹ <http://nedwww.ipac.caltech.edu>

² The *B* images are badly affected by a non-optimal focus.

Telescope	Date	Band	Exposure
<i>Magellan</i> Baade	2009 Aug 26	R	540 s
		V	540 s
<i>Swift</i> /UVOT	2008 Oct 24	U	380 s
		UVW1	760 s
	2008 Nov 01	U	730 s
		UVW1	1690 s
	2008 Nov 07	UVW2	2640 s
		U	1210 s
		UVW1	2410 s
	2008 Nov 14	UVW2	3860 s
		U	980 s
		UVW1	1960 s
	2009 Aug 05	UVW2	3810 s
		UVW2	9750 s
		UVW2	9130 s
		UVW2	5660 s
		UVW2	680 s
		UVW2	4260 s
		UVW2	2200 s
		UVW2	2200 s

Table 1. Optical/UV observation log.

2008 October and 2009 August. The total exposure times were 3.3 ks in the U band, 6.7 ks in $UVW1$, 4.9 ks in $UVM2$, and 42.0 ks in $UVW2$. In fact, the $UVM2$ exposure proved to be too short for meaningful analysis, and we do not use it further. See Table 1 for a log of our observations.

3 OPTICAL COUNTERPART OF HLX1

We used the STARLINK program *gaia*, as well as standard IRAF packages, to analyze the optical images. We calibrated the astrometry of the *Magellan* images by using stellar positions from the Guide Star Catalog Version 2.3 (Lasker et al. 2008). Our optical astrometry is accurate to $\approx 0''.3$.

At first inspection, any faint optical counterpart to the X-ray source would be swamped by the strong stellar light from the main galaxy (Figure 1). However, at closer inspection we noted that there is an excess of counts, consistent with a point source, in the R -band image at the position of HLX1. To visualize this source, at first we generated a Gaussian-smoothed R -band image and subtracted it from the original image. This brings up residuals consistent with point-like sources, including a source in the X-ray error circle of HLX1 (Figure 2, top panel). To get a better result, we took advantage of the fact that the galaxy is almost perfectly edge-on and its optical isophotes are very symmetrical above and below the disk plane near the position of HLX1; therefore, we folded the image over the disk plane, and subtracted one side of the galaxy from the other. This technique removes most of the “background” galactic light and reveals the HLX1 counterpart as a point-like source (Figure 2, bottom panel). The optical counterpart is located at RA = $01^h 10^m 28^s.25$, Dec = $-46^\circ 04' 22''.3$, which is $\lesssim 0''.3$ from the X-ray position. There are no other optical sources of comparable or higher brightness within several arcsec. As a further check that the optical source is not for example a cosmic ray, we analysed each of the three 180-s sub-exposures separately, and found it in each of them.

We performed an aperture photometry measurement of this source, and used isolated point-like objects in the field to calculate the aperture correction. To convert from count rates to fluxes, we used stars with photometric measurements in the USNO-B1.0 Catalog (Monet et al. 2003), as well as the exposure time calculator for the *Magellan* telescope. We obtain a brightness $R = 24.6 \pm 0.2$ mag. If the object is located in ESO 243-49, its intrinsic brightness (corrected for Galactic extinction and taking into account the distance uncertainty) is $M_R = -10.2 \pm 0.3$ mag. We repeated the same procedure with the V -band image. The source is only marginally detected at the same position. Taking into account the uncertainties in the background subtraction, we estimate a brightness $V = 25.4 \pm 0.3$ mag ($M_V = -9.5 \pm 0.3$ mag). In the B -band, the image quality is not good enough for us to draw any conclusions.

4 UV EMISSION FROM ESO 243-49

We retrieved the *Swift*/UVOT observations (datasets 00031287001 through 00031287010) from the HEASARC archive, and processed them using standard FTOOLS tasks. We verified the images in each filter for a successful aspect correction, then stacked and resampled them using *uvotimsum*. We checked the astrometry of the UVOT images by correlating sources also detected in the *Magellan* images, as well as AGN detected in the *XMM-Newton* images. We performed aperture photometry with *uvotsource* to derive initial count rates. Conversion factors between UVOT count rates and fluxes or magnitudes are detailed in Poole et al. (2008). However, those factors were derived for an aperture of $5''$ on point sources. In our case, we are also interested in the total emission from extended regions. Therefore, we calculated appropriate aperture corrections for extended emission, using the extended UVOT point-spread-function (Breeveld et al. 2009), and the appropriate HEASARC *Swift*/UVOT CALDB files.

We do not detect a point-like counterpart at the position of the ULX, with an upper limit $UVW2 \approx 22.2$ mag; this corresponds to a flux $f_\nu \approx 9.3 \times 10^{-7}$ Jy = 9.3×10^{-30} erg $s^{-1} cm^{-2} Hz^{-1}$ at an effective frequency of 1.477×10^{15} Hz, or $\approx 2030 \text{ \AA}$ (Poole et al. 2008). The non-detection of a point-like counterpart is not surprising, given that the full-width half-maximum of the point spread function is $2''.9$ for the $UVW2$ filter. However, the UVOT data provide interesting information on the host galaxy environment. For the whole galaxy, we measure a total brightness (uncorrected for extinction) $U = 15.7 \pm 0.2$ mag, $UVW1 = 17.1 \pm 0.2$ mag, $UVW2 = 18.06 \pm 0.12$ mag (3σ uncertainties). The $UVW2$ brightness corresponds to a flux $f_\nu = 4.49 \times 10^{-5}$ Jy = 4.49×10^{-28} erg $s^{-1} cm^{-2} Hz^{-1}$ at $\nu = 1.477 \times 10^{15}$ Hz.

First, we tested whether these brightnesses and colours are consistent with the moderately old population suggested by the optical colours. We ran continuous and instantaneous star-formation simulations with Starburst99 (Leitherer et al. 1999; Vazquez & Leitherer 2005). As a well-fitting example, we illustrate the case of a population with initial stellar mass = $4 \times 10^{10} M_\odot$, solar metallicity and single age of 3 Gyrs. At the distance of ESO 243-49 and after adding foreground extinction, this population is predicted to have $R \approx 13.6$ mag, $B \approx 15.0$ mag, $U \approx 15.6$ mag, $UVW1 \approx 17.0$ mag,

$UVW2 \approx 19.1$ mag. By comparison with our measured values, we infer that the emission in all bands up to $UVW1$ (effective wavelength 2634 \AA) is dominated by a moderately old stellar population, but extra UV emission from a much younger population dominates the $UVW2$ band. An ongoing star-formation rate $\approx 0.03 M_{\odot} \text{ yr}^{-1}$ is sufficient to explain the dominant far-UV emission, while it would have a negligible effect in the other bands, compared to the emission from the older population.

The presence of a young stellar population in the bulge of ESO 243-49 is directly visible from the $UVW2$ image (Figure 3). The emission is asymmetric, with an excess North East of the nucleus (the same sector as the HLX1). In order to quantify the degree of asymmetry, we used the highly symmetric R-band isophotes to define four quadrants (bounded by the galactic plane and the normal to the plane), and extracted the $UVW2$ flux in each of them. Expressing the excess in the four quadrants as a percentage of the mean, the excess is +15% in the North, -9% in the West, -1% in the East, and -5% in the South quadrant. The excess $UVW2$ emission in the North quadrant may be interpreted as a more recent or intense phase of star formation.

5 DISCUSSION

If the X-ray source HLX1 is proven to be an accreting BH with mass $\sim 10^3\text{--}10^4 M_{\odot}$, there would be important implications on models of galaxy formation and evolution. Identifying its optical counterpart gives a crucial constraint on its nature. We have found an unresolved optical source within its X-ray error circle, and it is likely to be physically associated to HLX1. Assuming a direct association, we obtain an X-ray/optical flux ratio, using the standard definition (Hornschemeier et al. 2001): $\log(f_X/f_R) = \log f_X + 5.5 + R/2.5$, where f_X is the intrinsic flux in the 0.3–10 keV band (taken from Godet et al. 2009, and our spectral analysis of the *Swift* X-Ray Telescope (XRT) data). We obtain $f_X/f_R \approx 1700\text{--}1900$ for the X-ray high state of 2009 August, only slightly depending on the choice of X-ray spectral model. This value is much higher than expected for AGN, which have typical $f_X/f_R \lesssim 10$ (Laird et al. 2009; Bauer et al. 2004). A number of distant, faint AGN are undetected in the optical band because of extinction, which should not be an issue for this object (Farrell et al. 2009; Godet et al. 2009). Besides, AGN with a 0.5–2 keV flux of $\approx 5 \times 10^{-13} \text{ erg s}^{-1} \text{ cm}^{-2}$ are rare ($N \approx 0.5 \text{ deg}^{-2}$; Hasinger 1998) and should have been identified in other bands. Physically, the X-ray/optical flux ratio of HLX1 is due to an X-ray spectrum dominated by a thermal component with characteristic temperature $\sim 0.2 \text{ keV}$, too high to be from the accretion disk of a supermassive BH. The red colour of the optical counterpart ($V - R = 0.8 \pm 0.4$) suggests that it is not dominated by the Rayleigh-Jeans tail of an accretion disk spectrum.

Neutron stars are a class of objects that can reach X-ray/optical flux ratios > 1000 , with thermal X-ray emission from their surface. An isolated neutron star is ruled out by the observed rapid state transitions (Godet et al. 2009). Therefore, we only need to consider accreting neutron stars with a faint low-mass companion. We note (Soria et al., in prep.) that the *Swift*/XRT spectrum of HLX1 in the high state can also be fitted with a neutron star atmosphere

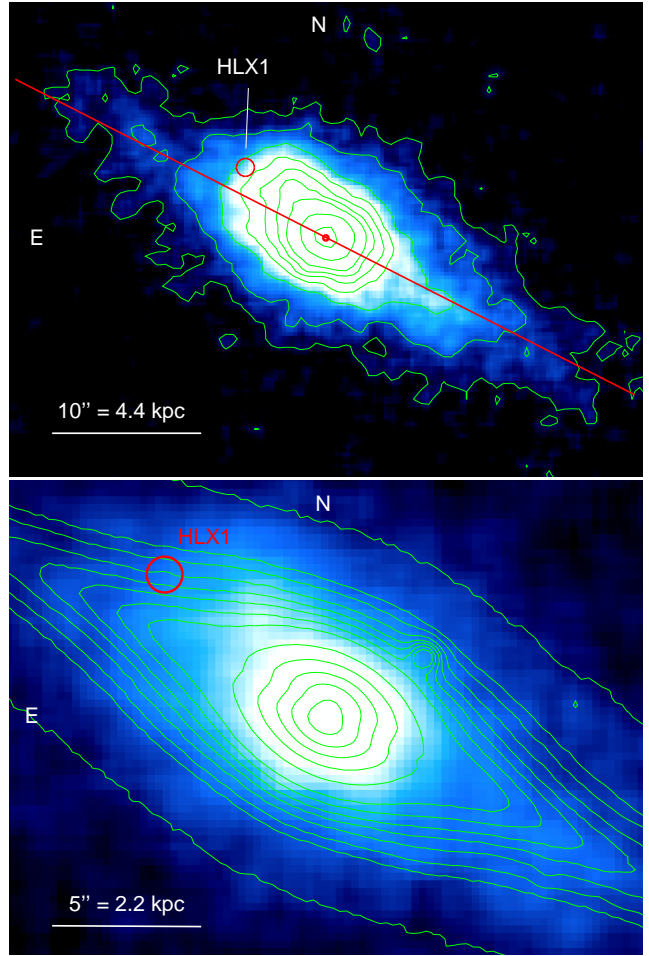


Figure 3. Top panel: *Swift*/UVOT image of the galaxy in the $UVW2$ band, with arbitrary flux contour levels. The position of HLX1 is marked with a red circle. We also marked the galactic plane (red line), and the position of the optical nucleus (red dot), from the Magellan images, which coincides with the UV nucleus. Bottom panel: zoomed-in $UVW2$ -band image, plotted with a different greyscale, to highlight the excess UV emission North East of the galactic nucleus. Contours are arbitrary flux levels from the Magellan R -band image, overplotted here to highlight the larger asymmetry of the UV emission.

model (e.g., `nsa` in XSPEC). If the thermal emission comes from the whole surface of the star (radius of 10 km), we will obtain a characteristic distance $\approx 2.5 \text{ kpc}$ corresponding to a 0.3–10 keV luminosity $\approx 7 \times 10^{32} \text{ erg s}^{-1}$, and reasonable values for the neutron star mass $\approx 1.5 M_{\odot}$ and temperature $\approx 0.1 \text{ keV}$. If HLX1 is a neutron star X-ray binary located at $\approx 2.5 \text{ kpc}$ in the Galactic halo, $R \approx 24.6 \text{ mag}$ implies $M_R \approx 12.6 \text{ mag}$, consistent with a main-sequence M5 star (initial mass $\approx 0.1 M_{\odot}$). A late-type M star is also consistent with the observed red colour. Thus, we cannot completely rule out the possibility of an accreting neutron star. In this case, the excess UV emission North East of the nucleus in ESO 243-49 is purely coincidental. However, the X-ray spectral state evolution has not been observed in any other quiescent neutron star X-ray binaries in this luminosity range.

The optical counterpart of HLX1 does not stick out like a unique object in the field. In the R -band image, we identified several globular clusters around ESO 243-49, with

comparable brightnesses. If the HLX1 counterpart is also a globular cluster in that galaxy, its optical luminosity would place it between the Milky Way globular clusters ω Cen ($M_V = -10.3$ mag, $M_R = -10.8$ mag, $M_{\text{tot}} \approx 2.8 \times 10^6 M_\odot$) and 47 Tuc ($M_V = -9.4$ mag, $M_R = -10.0$ mag, $M_{\text{tot}} \approx 1.1 \times 10^6 M_\odot$) (Harris 1996; van der Marel & Anderson 2009). It would be slightly smaller than the Andromeda cluster G1 ($M_V = -11.2$ mag, $M_R = -11.8$ mag, $M_{\text{tot}} \approx 5 \times 10^6 M_\odot$; Graham & Spitler 2009), which is a strong candidate for the presence of an $\approx 2 \times 10^4 M_\odot$ BH (Gebhardt et al. 2005). There are a number of scenarios for the formation of an intermediate-mass BH inside a massive star cluster. In a young star cluster, runaway core collapse and coalescence of the most massive stars can occur over a timescale $\lesssim 3$ Myrs and can result in the formation of a supermassive star, which can quickly collapse into a BH (Portegies Zwart & McMillan 2002; Freitag et al. 2006). In an old globular cluster, an intermediate-mass BH can be formed from the merger of stellar-mass BHs and neutron stars over a timescale $\sim 10^9$ yr (O’Leary et al. 2006).

The most intriguing scenario is that some massive star clusters may have been the nuclear clusters of satellite galaxies accreted and tidally disrupted by a more massive galaxy. Dwarf galaxies are the most common type of galaxies in clusters (e.g., Binggeli et al. 1985) and many of them are nucleated (e.g., Graham & Guzman 2003; Côté et al. 2006). In many cases, a nuclear cluster may coexist with a nuclear BH (Graham & Spitler 2009; Seth et al. 2008). This may end up in the halo of a bigger galaxy after a merger. ω Cen itself may have originated from the nuclear star cluster of an accreted dwarf (Bekki & Freeman 2003). Similar suggestions have been made for a group of clusters in NGC 5128 (Peng et al. 2002; Chattopadhyay et al. 2009). The recent or ongoing star formation that we have found in ESO 243-49 (Section 4) may have been triggered by the passage and tidal disruption of the satellite galaxy, roughly along the South-West to North-East direction. HLX1 is located ≈ 1 kpc (in projection) ahead of the North East plume of UV emission. However, this is not inconsistent with the previous scenario, as the peak in the far-UV emission occurs ≈ 3 –4 Myrs after the initial star-formation trigger, owing to the time necessary for the molecular gas to collapse into stars, and then for the most massive stars to evolve towards the blue supergiant stage. During that time, the stripped nucleus and its BH may have travelled ~ 1 kpc at a projected speed ≈ 400 km s $^{-1}$ (a plausible value for a dwarf galaxy encounter).

In summary, we have identified an optical counterpart for HLX1 in ESO 243-49 in the *Magellan* images. The optical brightness and colour are consistent with a massive star cluster in ESO 243-49. The galaxy is dominated by a ~ 2 –5 Gyr old population, but shows excess emission in the *Swift*/UVOT *UVW2* band, consistent with a recent episode of star formation. The far-UV emission has an asymmetric shape and is stronger roughly in the direction of HLX1.

ACKNOWLEDGMENTS

We thank Mark Cropper, Rosanne di Stefano, Sean Farrell, Jeanette Gladstone, Craig Heinke, Erik Hooverstein, Tom Maccarone, Greg Sivakoff, Lee Spitler and Doug Swartz for discussions.

REFERENCES

- Bauer, F. E., Alexander, D. M., Brandt, W. N., Schneider, D. P., Treister, E., Hornschemeier, A. E., & Garmire, G. P. 2004, *AJ*, 128, 2048
- Bessell, M. S. 1979, *PASP*, 91, 589
- Bekki, K., & Freeman, K. C. 2003, *MNRAS*, 346, L11
- Binggeli, B., Sandage, A., & Tammann, G. A. 1985, *AJ*, 90, 1681
- Breeveld, A.A., et al. 2009, *MNRAS*, submitted
- Caldwell, N., & Rose, J. A. 1997, *AJ*, 113, 492
- Chattopadhyay, A. K., Chattopadhyay, T., Davoust, E., Mondal, S., & Sharina, M. 2009, *ApJ*, in press (arXiv0909.4161)
- Côté, P., et al. 2006, *ApJS*, 165, 57
- Davis, D. S., & Mushotzky, R. F. 2004, *ApJ*, 604, 653
- Farrell, S. A., Webb, N. A., Barret, D., Godet, O., & Rodrigues, J. M. 2009, *Nature*, 460, 73
- Feng, H., & Kaaret, P. 2009, *Science*, in press
- Freitag, M., Gürkan, M. A., & Rasio, F. A. 2006, *MNRAS*, 368, 141
- Gebhardt, K., Rich, R. M., & Ho, L. C. 2005, *ApJ*, 634, 1093
- Godet, O., Barret, D., Webb, N. A., Farrell, S. A., & Gehrels, N. 2009, *ApJL*, in press (arXiv0909.4458)
- Graham, A. W., & Guzmán, R. 2003, *AJ*, 125, 2936
- Graham, A. W., & Spitler, L. R. 2009, *MNRAS*, 397, 2148
- Grimm, H.-J., Gilfanov, M., & Sunyaev, R. 2003, *MNRAS*, 339, 793
- Harris, W. E. 1996, *AJ*, 112, 1487
- Hasinger, G. 1998, *AN*, 319, 37
- Hornschemeier, A. E., et al. 2001, *ApJ*, 554, 742
- King, A. R. 2009, *MNRAS*, 393, L41
- Laird, E. S., et al. 2009, *ApJS*, 180, 102
- Lasker, B. M., et al. 2008, *AJ*, 136, 735
- Leitherer, C., et al. 1999, *ApJS*, 123, 3
- Li, J.-T., Li, Z., Wang, Q. D., Irwin, J. A., & Rossa, J. 2008, *MNRAS*, 390, 59
- Monet, D. G., et al. 2003, *AJ*, 125, 984
- O’Leary, R. M., Rasio, F. A., Fregeau, J. M., Ivanova, N., & O’Shaughnessy, R. 2006, *ApJ*, 637, 937
- Peng, E. W., Ford, H. C., Freeman, K. C., & White, R. L. 2002, *AJ*, 124, 3144
- Poole, T.S., et al. 2008, *MNRAS*, 383, 627
- Portegies Zwart, S. F., & McMillan, S. L. W. 2002, *ApJ*, 576, 899
- Roberts, T. P. 2007, *Ap&SS*, 311, 203
- Schlegel, D. J., Finkbeiner, D. P., & Davis, M. 1998, *ApJ*, 500, 525
- Seth, A., Agüeros, M., Lee, D., & Basu-Zych, A. 2008, 678, 116
- Swartz, D. A., Ghosh, K. K., Tennant, A. F., & Wu, K. 2004, *ApJS*, 154, 519
- van der Marel, R. P., & Anderson, J. 2009, *ApJ*, submitted (arXiv0905.0638)
- Vazquez, G. A., & Leitherer, C. 2005, *ApJ*, 621, 695
- Wolter, A., Trinchieri, G., & Colpi, M. 2007, *MNRAS*, 373, 1627
- Yungelson, L. R., van den Heuvel, E. P. J., Vink, J. S., Portegies Zwart, S. F., & de Koter, A. 2008, *A&A*, 477, 223